www.amlett.com, www.vbripress.com/aml, DOI: 10.5185/amlett.2016.xxxx Published online by the VBRI Press in 2016

A study on thermal and optical properties of glycine sodium nitrate crystals

Authors: M. P. Deshpande[1], Vivek P. Gujarati[*1], Kiran N. Patel, S.H. Chaki[1]

1: Department of physics, Sardar Patel University, Vallabh Vidyanagar, 370001, India.

[*]Email: vivekgujarati@gmail.com

Received: --/--/2016, Revised: --/--/2016 and Accepted: --/--/2016

ABSTRACT

Abstract: Crystals of Glycine with Sodium Nitrate (GSN) taken in concentration ratio of 1:1 were grown by slow evaporation technique. Solubility of the material was determined in double distilled water at different temperatures. Purity of the grown crystal was checked by CHN and EDAX analysis whereas crystalline nature was confirmed from powder X-ray diffraction pattern. Dielectric study of the sample was carried out between the frequency range 1Hz to 100 KHz. FTIR spectra along with Raman spectra was used to look at the presence of different chemical bonds and groups present. Optical absorption spectra recorded in UV-Vis (250-800nm) region for the GSN crystal was analyzed to determine the optical energy bandgap of the sample. GSN crystal was thermally investigated between 323-773 K at three different heating rates (5, 10, 15 K/min) and activation energy was computed using Kissinger method.

Keywords: Crystal; Dielectric; TGA/DSC.

Introduction

The research field of non-linear optics (NLO) investigates new materials which can satisfy the modern society's demand for photonics and telecommunication. These materials with high second harmonic generation efficiency can be used to construct optical devices like frequency doublers, active optical interconnects, switches and optical modulators [1-2]. Amino acids are important NLO material because of the fact that they possess chiral symmetry, a proton donating carboxyl (-COOH) group and a proton accepting amino ($-NH_2$) group [3]. It can form many different complexes with many organic and inorganic compounds [4] like, L-arginine hydrochloride, L-histidine tetrafluoroborate, L-alanine tetrafluoroborate, L-histidine bromide [5-8], etc. In this class of semi-organic crystals the weak forces of organic solids are replaced by stronger ionic forces and form a complete new class of semi-organic materials [9]. In the present work, attempts have been made to crystallize and grow crystals of glycine with sodium nitrate from aqueous solution at room temperature in equimolar ratio. The reason for adding sodium nitrate is to produce crystal with improved thermal and mechanical properties as compared to other pure organic/semi-organic materials in order to recognize it as candidate for the various applications where it can be used at higher temperatures. In this paper, we have reported the growth of glycine sodium nitrate (GSN) crystals and its investigation by different characterization techniques such as CHN, EDAX, Powder XRD, UV-Vis, FTIR, Raman spectroscopy, dielectric measurements and TGA/DSC.

Solubility and Growth

Solubility of the glycine sodium nitrate crystal was checked in double distilled water at different temperatures. Figure 1 shows the plot of solubility of material in 50ml water at different temperatures. From Figure 1 it is seen that solubility varies linearly with temperature upto 60 ^{0}C. If solubility is too high then it is difficult to grow bulk single crystals and if it is too small then it restricts the size and growth rate of the crystals [10]. Glycine sodium nitrate (GSN) crystals were grown using slow evaporation method. Glycine and sodium nitrate were taken in the molar ratio of 1:1. Solution was prepared in double distilled water and filtered using Whatman filter paper. Then this solution was filled in petri dish and covered by parafilm and then kept in vibration free housing in order to get good quality crystals. Figure 2 shows the photograph of as grown GSN crystals.

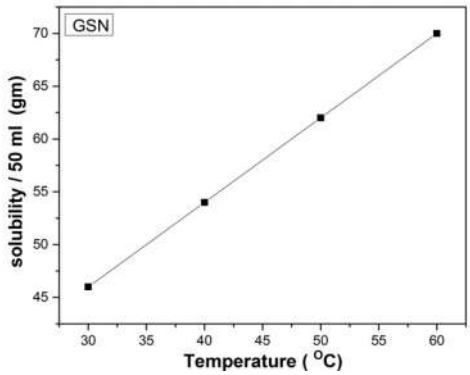

Figure 1: Solubility curve


Figure 2: As grown GSN crystals

Results and discussion

CHN and EDAX

CHN and EDAX (Energy Dispersive Analysis of X-rays) analysis were carried out to authenticate the presence of chemical elements like carbon, hydrogen, nitrogen and sodium. From these analysis we observed that no other impurity elements were present in the grown crystals.

Powder XRD

Bruker D8 Advance X-ray diffractometer was employed to record powder X-ray diffraction pattern of the grown crystal. Diffraction pattern was indexed based on monoclinic system by Powder-X software and the lattice parameter were taken as a=14.323 Å, b=5.2573 A, c=9.1156 Å and β=119.030 with space group Cc [11-13]. Powder X-ray diffractogram of GSN crystal shown in Figure 3 indicates good crystalline nature as seen from the strong and sharp diffraction peaks.

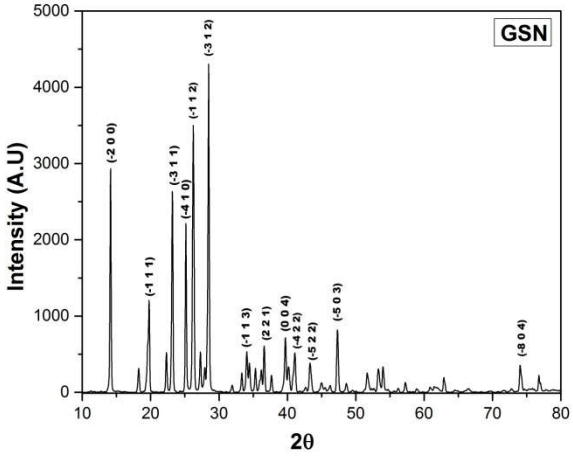

Figure 3: Powder X-ray diffractogram of GSN crystal

Dielectric study

New crystals with low dielectric constant are required in microelectronic industries as interlayer dielectric (ILD) [17]. To check dielectric property initially crystal is powdered and then uniform size pellets were prepared. For dielectric measurements this pellet are placed between two copper electrodes and then measurements were carried out between the frequency range 1 Hz to 100 KHz. Fig. 4(a) shows the variation of dielectric constant and dielectric loss with change in frequency. All four polarizations namely dipolar, ionic, electric and space charge are contributing to the larger value of dielectric constant at lower values of frequencies [14-16]. At higher values of frequencies dielectric constant becomes independent function of frequency. The variation of $\sigma_{a.c.}$ (a.c. conductivity) with log f for GSN sample is plotted as shown in Fig 4(b). We calculated the $\sigma_{a.c.}$ using the relation $\sigma_{a.c.} = 2\pi f (\tan \delta) \varepsilon_0 \varepsilon_r$, where f is the frequency.

Raman and FTIR

Raman Spectra of GSN crystal was recorded using Jobin Yvon Horibra LABRAM-HR micro Raman system from 200-2000 cm^{-1} using Argon laser (488 nm) source. The Raman spectra is shown in figure 5(a) whereas FTIR spectra is shown in figure 5(b) recorded by Perkin Elmer Spectrum GX from 400-4000 cm^{-1}. The comparative chart of different vibrational modes observed in Raman and IR spectra is shown in Table 1.

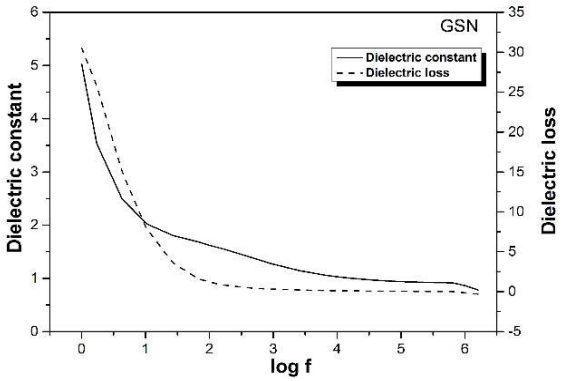

Figure 4(a): log f vs. dielectric constant and dielectric loss

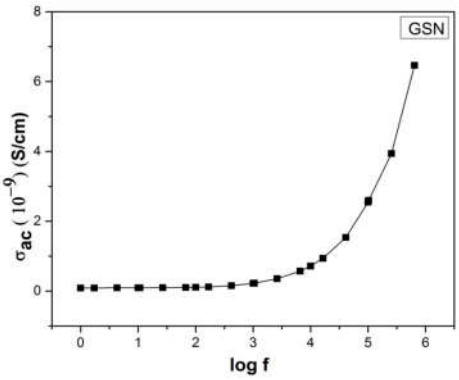

Figure 4(b): log f vs. a.c. conductivity

Table 1: Vibrational modes assigned by Raman and FTIR spectra

Raman (cm^{-1})	FTIR (cm^{-1})	Assignment
390.47		NH_3^+ Torsion
506.16	507.46	COO^- Rocking
582.12	587.07	COO^- Deform
678.72	676.42	NO_3^- In plane Deformation
720.79		COO^- Deform
899.97	892.03	C-C stretch
	937.10	CH_2 Rocking
1052.28	1038.88	NO_3^- Symmetric stretch
	1116.72	NH_3^+ Rocking
	1136.0	CH_2 Twisting
1333.13	1335.78	CH_2 Wagging
1373.25	1384.27	NO_3^- Asymmetric stretch
1452.71	1449.47	CH_2 Scissoring
1512.31	1508.44	NH_3^+ Symmetric Bending
1614.36	1619.75	NH_3^+ Asymmetric Bending
1660.36		Overtones
	2627.48	Overtones
	2718.21	Overtones

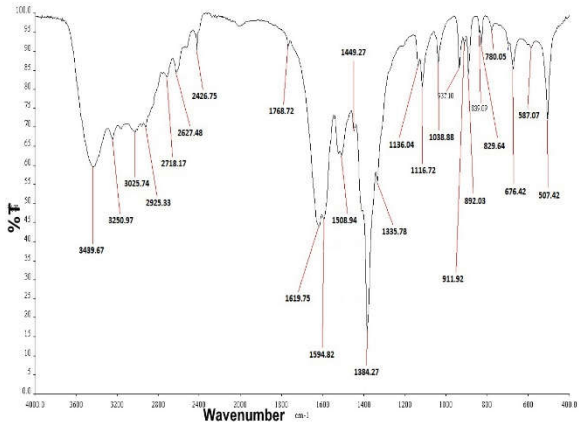

Figure 5(a): FTIR spectra of GSN crystal

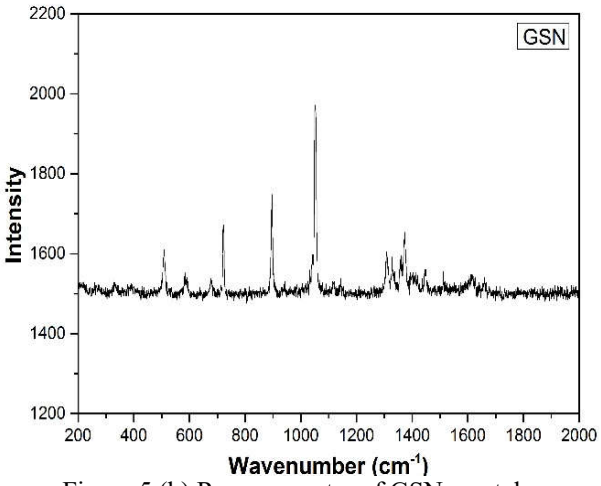

Figure 5 (b) Raman spectra of GSN crystals

UV-Vis spectroscopy

Figure 6(a) shows optical absorption spectra recorded between 250-800nm using Perkin Elmer Lambda 19 showing UV cut off for GSN crystal near 300nm, which matches well with reported data [18-19]. The optical energy bandgap value comes out to be 3.57eV which indicates the dielectric behavior of the crystal as calculated from the plot of $(\alpha h\nu)^2$ vs. hν as shown in figure 6(b) [20]. The excellent transmission observed in the visible region suggest that the property of a crystal is desirable for optoelectronic applications [21].

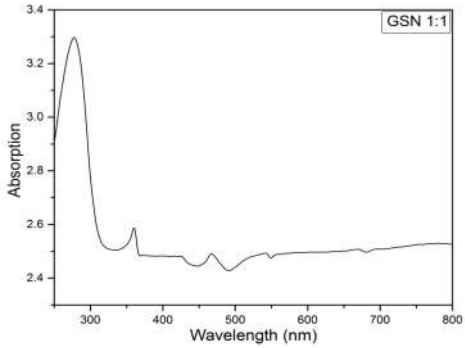

Figure 6 (a): UV-Vis absorption spectra

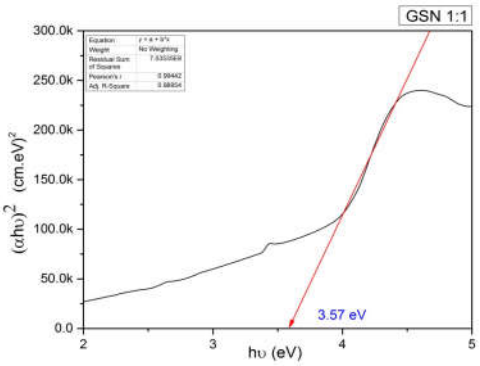

Figure 6(b): Plot of $(\alpha h\nu)^2$ vs. hν

TGA/DSC

Figure 7 is showing TGA/DSC curves for GSN crystal studied using PerkinElmer Pyris thermal analyzer between 323-773K at three different heating rates (5, 10, 15 K/min). Good thermal stability of the crystal was observed from the DSC plot, which indicates that crystal is stable upto 485-492 K because endothermic peaks were not observed, which characterize crystalline transformations. The activation energy is the difference in energy content between the activated or transition state configuration and the reactant their initial configuration, as per transition-state theory [22]. The Kissinger method was used to calculate the activation energy for the GSN crystal which comes out to be average 251.8 kJ/mole. After the evaluation of Activation Energy and Pre-Exponential factor (A) from Kissinger model, various thermal parameters like Entropy (ΔS), Enthalpy (ΔH) and Gibbs free energy (ΔG) were calculated using the equations (1), (2) and (3) respectively and are shown in Table 2.

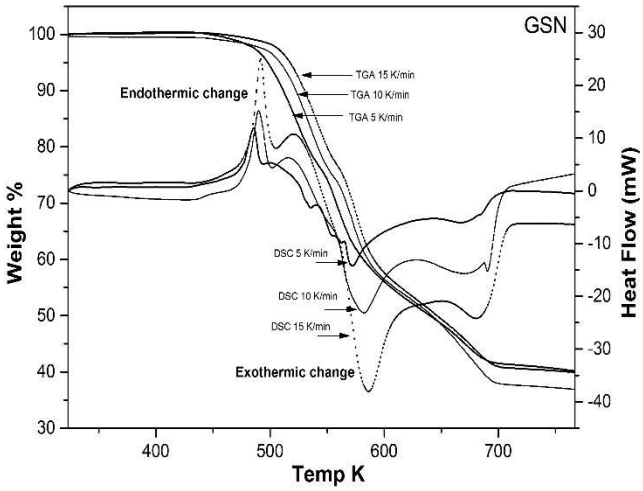

Figure 7: TGA/DSC curve

$$S = 2.303 \times R \times \log \frac{Ah}{K_b T} \quad (1)$$

$$H = E \quad RT \quad (2)$$

$$G = \quad H \quad T \ \ S \quad (3)$$

where, R = Universal gas constant, h = Planck's constant, and K_b= Boltzmann constant

Value of enthalpy (ΔH) was also calculated by finding area under the peaks in DSC curve which is shown in Table 2. For the exothermic peak negative value of Gibbs free energy (ΔG) indicates the good stability of the crystal. Value of Heat capacity C_p was also calculated from DSC plot, in the region of 323-450 K, which comes out to be 0.150, 0.121, and 0.099 mW/K for three different heating rates 5, 10 and 15 K/min respectively.

Table 2: Calculated thermal parameters

	ΔS J/mole K	ΔH kJ/mole	ΔH kJ/mole (from area under DTA curve)	ΔG kJ/mole	Activation Energy E kJ/mole	Linear correlation factor (R^2)
Endothermic Peak	475.07	293.97	287.29	41.39	298.39	0.980
Exothermic Peak	712.13	200.78	276.64	-177.82	205.20	0.979

Conclusion

GSN semi-organic crystals were grown at ambient temperature by the slow evaporation method. Good quality, optically clear crystals were obtained within 5-6 weeks' time. Purity of the material was checked by EDAX and CHN. From the reported data indexing was done to obtain powder X-ray diffractogram and very sharp peaks in diffractogram shows highly crystalline nature of the sample. The various vibrational groups associated with this crystal were studied using Raman and FTIR. Optical energy bandgap value was calculated using plot of $(\alpha h)^2$ vs. h and it comes out to be 3.57eV. Crystal showed excellent transparency in visible region of the spectrum which is good for opto-electric applications. Grown crystal has low dielectric constant at higher values of frequency, which is required in microelectronic industries as interlayer dielectric (ILD). No significant weight loss was observed in TGA curve observed before 485-492 K which indicates good thermal stability of the crystal.

Acknowledgements

We like to acknowledge IUC-DAE consortium for scientific research (Indore) for analyzing our sample by Raman, Powder XRD and Dielectric measurements, and SICART (Vallabh Vidyanagar) for doing UV-Vis and FTIR spectra of the sample.

References

[1] Willams D. J.; A.W. Chem. Int. Edition in Eng., 1984, 23,690.
DOI: 10.1002/anie.198406901

[2] Hernandez-Paredes J.; et.al; J. of Phys. and Chem. of Solids, **2008**, 69, 1974.
DOI: 10.1016/j.matlet.2007.11.059

[3] Lydia Caroline M.; Vasudevan S.; Mater. Lett., **2008**, 62, 2245.
DOI: 10.1016/j.jpcs.2008.02.010

[4] Phase Transitions, **2014.**
DOI: 10.1080/01411594.2014.953951

[5] Rashkovich L. N.; Yu Shekunov B.; J. Cryst. Growth, **1991,** 112**,** 183.
DOI: 10.1016/0022-0248(91)90923-S

[6] Aggarwal M. D.; Choi J.; Wang W.S.; Bhat K.; Lal R.B.; Shields A. D.; Penn B.G.; Fraizer D.O.; J. of Cryst. Growth, **1999**, 204, 179.
DOI: 10.1016/S0022-0248(99)00200-6

[7] Rajan Babu D.; Jayaraman D.; Mohan Kumar R.; Jayavel R.; J. Cryst. Growth, **2002,** 245, 121.
DOI: 10.1016/S0022-0248(02)01708-6

[8] Ittyachan R.; Sagayaraj P.; J. Cryst. Growth, **2003,** 249, 557.
DOI: 10.1016/S0022-0248(02)02116-4

[9] Varalakshmi S.; Ravi Kumar S. M.; Elango G.; Ravisankar R.; Spect. Acta Part A, **2014**, 133, 677.
DOI: 10.1016/j.saa.2014.06.038

[10] Dongare S. S. V.; Crystal growth and physical behavior of glycine metal salts as potential NLO materials, **2011.**

[11] Linet, J. M.; Das, S. J. Optik. **2012**, 123, 1895.
DOI: 10.1016/j.ijleo.2012.03.076

[12] Krishnakumar, R. V.; Nandhini, M. S.; Natarajan, S.; Sivakumar, K.; Varghese, C. B., Acta Crystal. **2001**, *C57*, 1149.
DOI: 10.1107/S0108270101011520

[13] Smolin, Y. I.; Lapshin, A. E.; Pankova, G. A., J. of Struct. Chem., **2007**, *48*, 708.
DOI: 10.1007/s10947-007-0106-9

[14] Saucedo E.; Fornaro L.; Corregidor V.; Dieguez E.; Eur. Phys. J. Appl. Phys., **2004**, 27, 427.
DOI: 10.1051/epjap:2004142

[15] Dharmaprakash S. M.; Mohan Rao P.; J. Mater. Sci. Lett., **1989**, 8, 1167.
DOI: 10.1007/BF01730058

[16] Rao K. V.; Smakula A.; J. Appl. Phys., **1965**, 36**,** 2031.
DOI: 10.4236/jmmce.2011.1013095

[17] Hatton B. T.; et.al, Mater. Today, **2006**, 9, 22.
DOI: 10.1016/S1369-7021(06)71387-6

[18] Linet J. M.; Das S. J.; Optik, **2012,** 123, 1895.
DOI: 10.1016/j.ijleo.2012.03.076

[19] Venkatraman V.; Maheswaran S.; Sherwood J. N.; Bhat H. L.; J. of Cryst. Growth, **1997**, 179, 605.
DOI: 10.1016/S0022-0248(97)00137-1

[20] Gujarati V. P.; Deshpande M. P.; Patel K.; Chaki S. H.; International Letters of Chemistry, Physics and Astronomy, **2015**, 61, 12.
DOI: 10.18052/www.scipress.com/ILCPA.61.12

[21] Suresh S.; Ramanand A.; Jayaraman D.; Navis Priya S. M.; Anand K.; Int. J. of Phys. Sci., **2011,** 16, 3875.
DOI: 10.5897/IJPS10.405

[22] Renate M. R. W.; Eduardo L. C.; Polymer Testing., **2014**, 40, 33.
DOI: 10.1016/j.polymertesting.2014.08.008

